

Supporting Information

for

Experimental and Theoretical Determination of the Role of Ions in Atomic Layer Annealing

Scott T. Ueda¹, Aaron McLeod², Youhwan Jo³, Zichen Zhang¹, Jacob Spiegelman¹, Jeff Spiegelman⁴, Dan Alvarez⁴, Daniel Moser⁵, Ravindra Kanjolia⁵, Mansour Moinpour⁵, Jacob Woodruff⁵, Kyeongjae Cho³, and Andrew C. Kummel^{2}*

¹*Materials Science and Engineering Program, University of California, San Diego, La Jolla, California 92093, USA*

²*Department of Chemistry and Biochemistry, University of California, San Diego, La Jolla, California 92093, USA*

³*Department of Materials Science and Engineering, University of Texas at Dallas, Richardson, Texas 75080, United States*

⁴*Rasirc, Inc., San Diego, CA 92126, USA*

⁵*EMD Performance Materials, Haverhill, MA 01832, USA*

**Corresponding Author: akummel@ucsd.edu*

Chamber Diagram

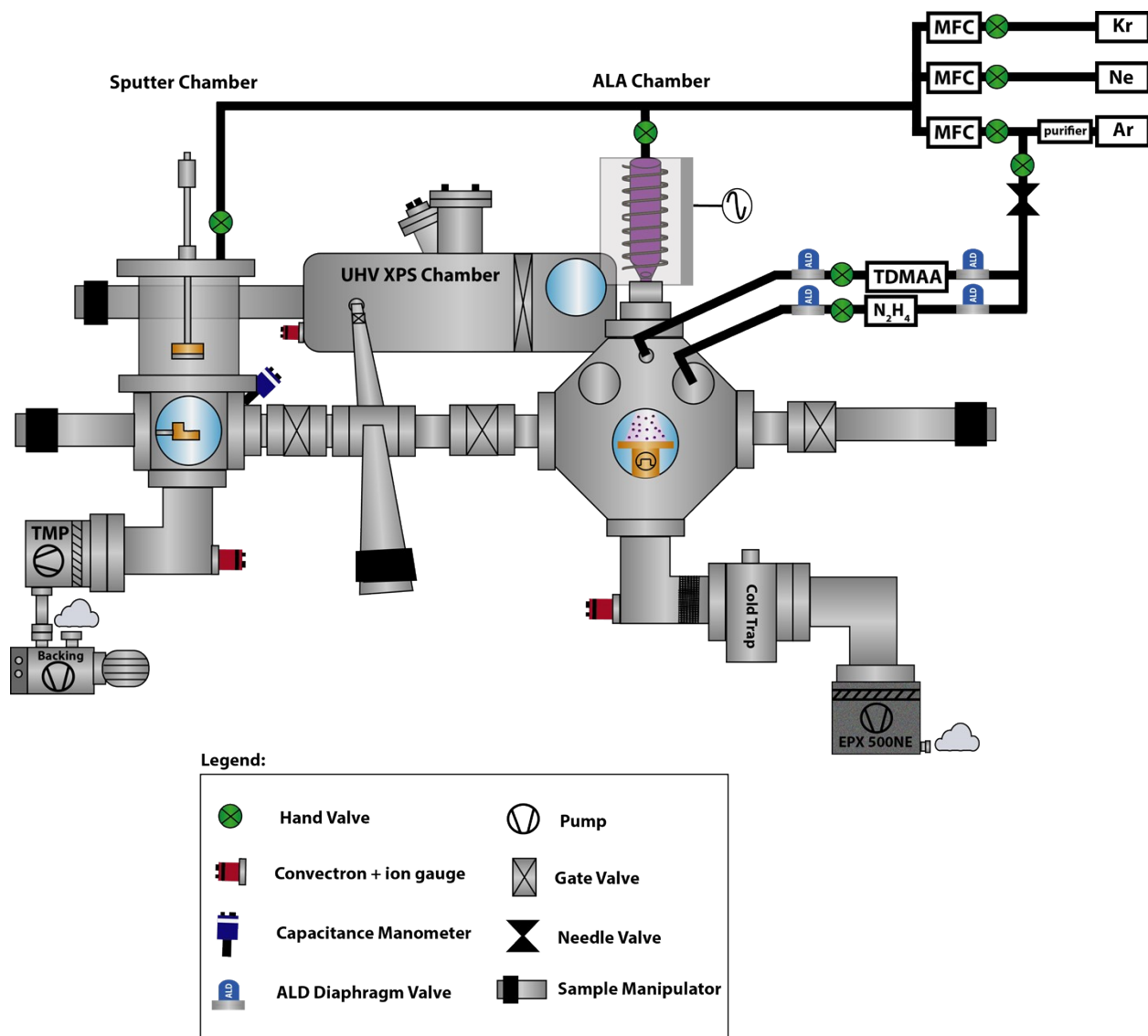


Figure S1. Schematic diagram of the custom deposition chamber used for the experiments. Deposition was carried out in a custom-built ALA system load locked into a commercial UHV tool capable of performing XPS. A sputtering chamber is also connected to this system but was not used in these experiments.

ALA treatment time optimization study

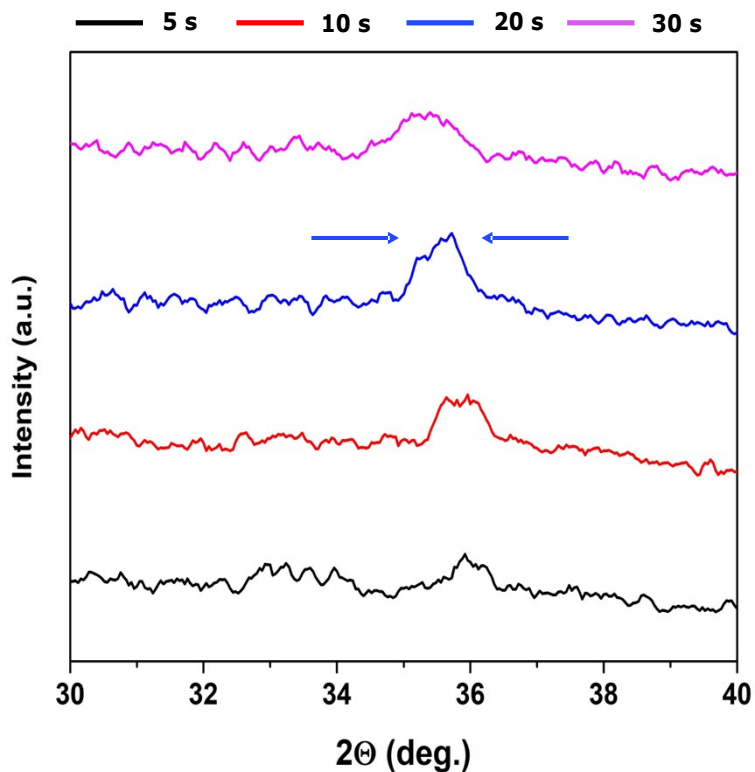


Figure S2. GIXRD scans for various ALA treatment times. Using Ar at -25 VDC, a 5 s ALA treatment (black) was found to induce negligible crystallinity. At 10 s treatment time (red), the AlN (002) diffraction peak begins to grow in intensity until it reaches a maximum at 20 s treatment time (blue). At 30 s treatment time (magenta), peak intensity decreases and the FWHM begins to broaden as compared to the optimal 20 s condition.

Electrical Characterization of ALA AlN Films

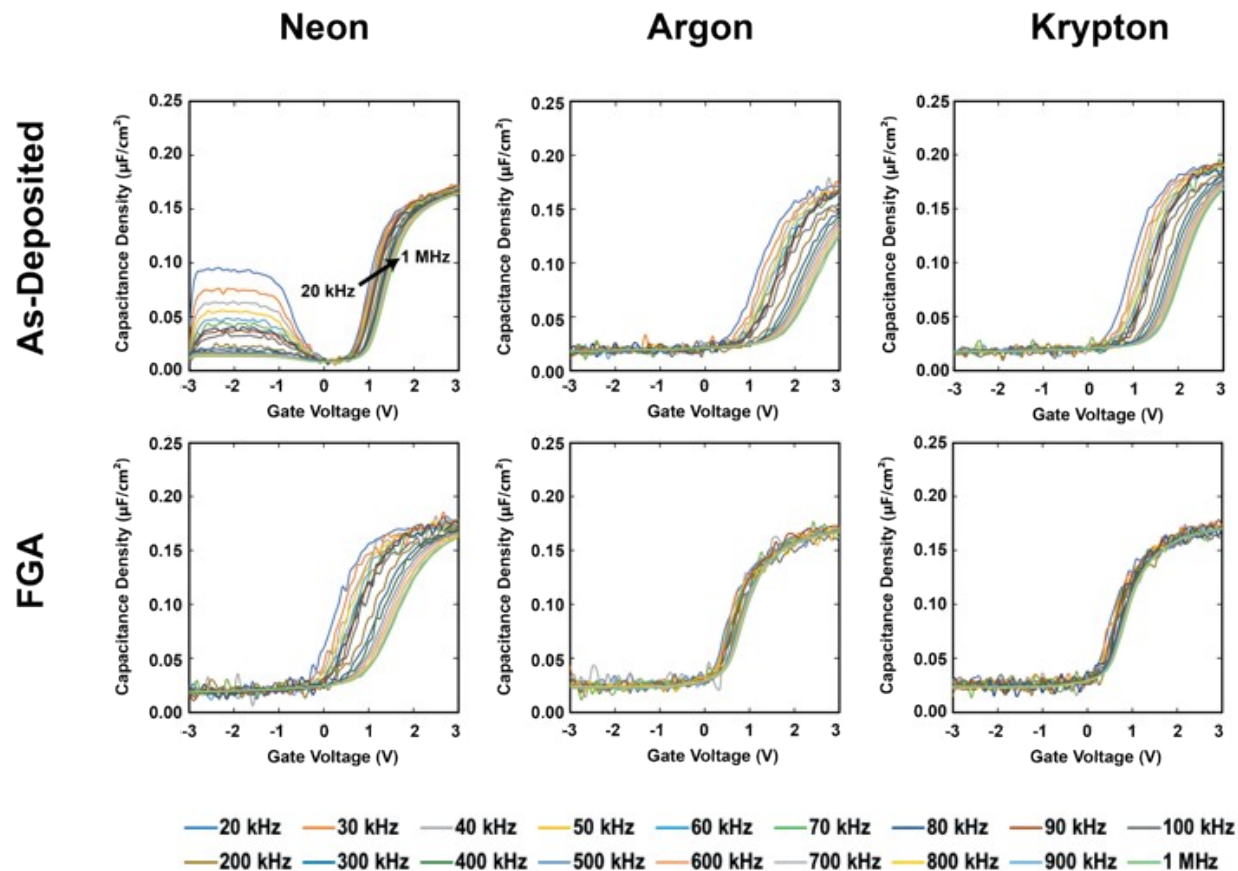


Figure S3. Capacitance-Voltage (C-V) characterization of ALA AlN samples deposited at the -40 V condition before and after forming gas anneal (FGA). C-V data before forming gas anneal indicate the highest defect density for the film deposited using Ne (see inversion in depletion) with the film deposited using Kr being the best in terms of both frequency dispersion as well as threshold voltage shift. After forming gas anneal, the samples deposited using Ar and Kr are nominally similar while the sample deposited using Ne continued to display a high defect density as evidenced by the frequency dispersion.

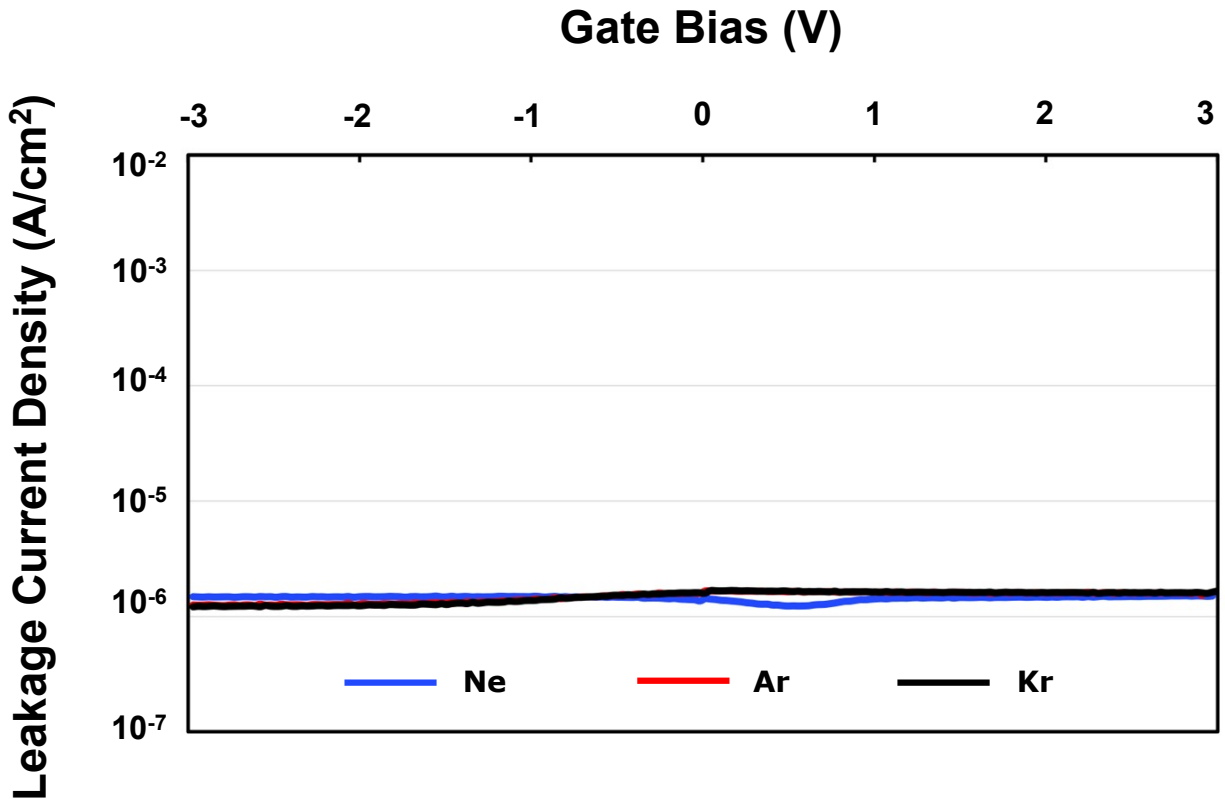


Figure S4. Current-Voltage (I-V) characterization of ALA AlN samples deposited at the -40 V condition before forming gas anneal (FGA). I-V data before forming gas anneal indicate no significant difference between the three samples as the leakage current is at the measurement limit for the system used. This is consistent with the ability to deposit highly insulating films regardless of ALA treatment gas used.

High-resolution XP spectra

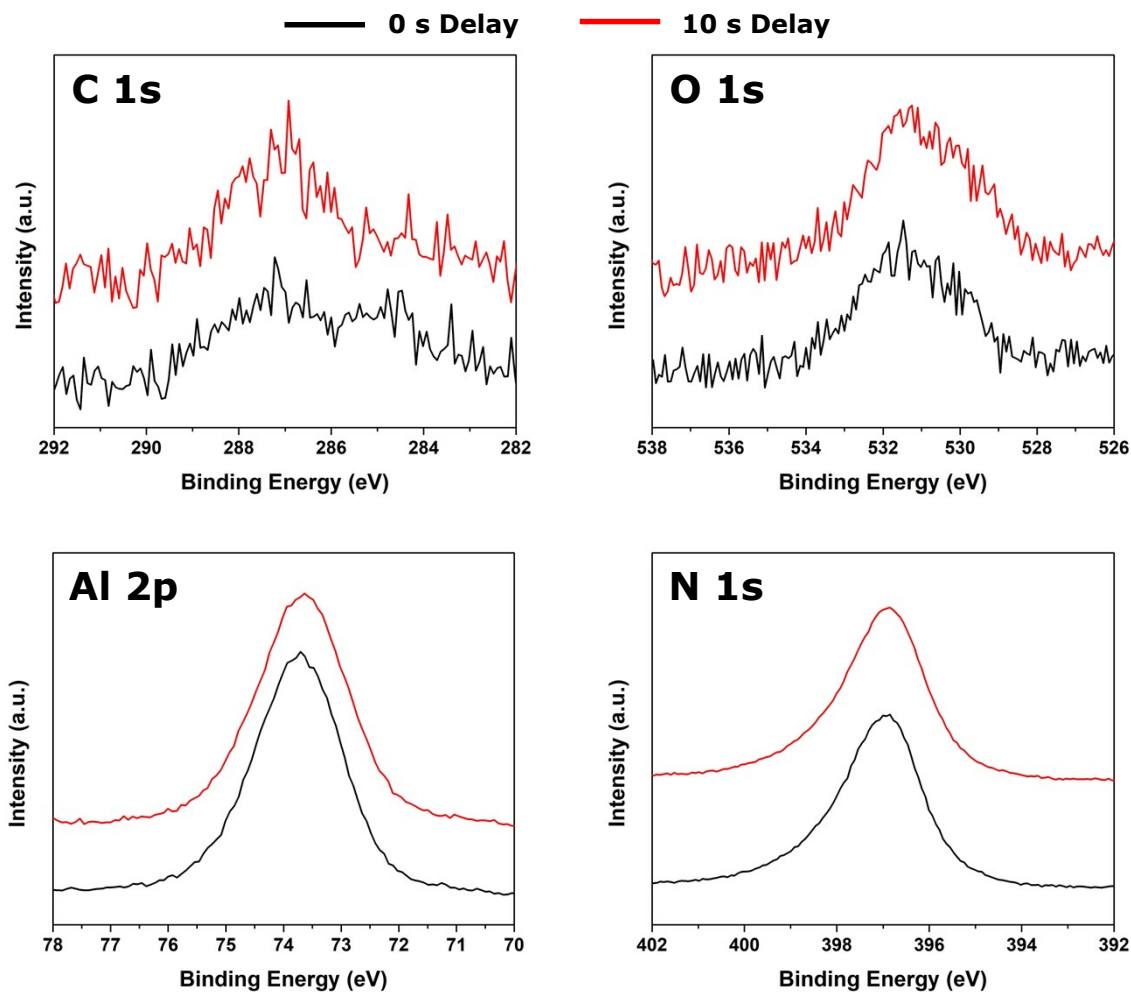


Figure S5. High-resolution XP Spectra for ALA with 0 s delay and 10 s delay. XPS data indicate the chemical composition for ALA with 0 s delay (black) and 10 s delay (red) is nearly identical. Oxygen and carbon contamination is similar and chemical shift data for both Al and N are identical and consistent with the formation of AlN.

Simulation

	ϵ (eV)	σ (Å)
N-Ne	0.01550981	2.47753403
N-Kr	0.01522095	3.20746499
Al-Ne	0.05331229	2.56834093
Al-Kr	0.06176949	3.23427089

Table S1. Parameter Values for Lennard-Jones Potential. Well depth (ϵ) and van der Waals radius (σ) parameter values used in the ion impact simulation. Values were calculated using the Waldman-Hagler mixing rule.